Project of Strategic Interest NEXTDATA

WP1.7

D1.7.C – Ensemble di modelli empirici e deterministici per siti LTER specifici e per specie animali campione

Antonello Provenzale (CNR IGG)
Marta Magnani (CNR IGG)
Simona Imperio (ISPRA)

This Deliverable describes some of the deterministic (process-based) and empirical (data-driven) ecosystem and population dynamics models developed and/or implemented during the NextData project, tuned for application to the Gran Paradiso Long-Term Ecological Research Site. All models are available upon request to info@nextdataproject.it.

1. Models for Alpine lake ecosystems

(Antonello Provenzale, CNR IGG; Jost von Hardenberg, CNR ISAC)

The model proposed here includes six compartments, describing the concentration of nutrients N (mainly phosphorus), two compartments of phytoplankton (P_1 and P_2), one zooplankton compartment (Z, mainly Daphnia), planktivorous fish (F), and piscivorous predator fish (C). For a general introduction to mathematical models in ecology see Kot (2001), for an introduction to lake ecology see Wentzel (2001) and for a discussion of phytoplankton ecology see Reynolds (2006). For NPZ models and their use in describing aquatic ecosystems see Bracco et al. (2000), Martin et al. (2002), Pasquero et al. (2005), Koszalka et al. (2007) and references therein.

All variables are measured in terms of concentrations, i.e., mass per unit volume. The concentration of N is given in phosphorus content, while the plankton and fish compartments are measured in carbon content (or biomass, to be decided). We then use the appropriate conversion factor in the form of fixed P:C (or P:biomass) ratio Q to convert from carbon (or biomass) to phosphorus. For simplicity, we assume Q to be the same for all organisms. Hereinafter, the subscript 1 and 2 refer to the two phytoplankton compartments, Z to the zooplankton and F and C to two compartments of fish. In the model, the nutrient is measured in μg-P/L, while phytoplankton, zooplankton and fish are measured in μg-C/L. Here P stands for Phosphorus and C for Carbon.

We do not explicitly describe the dynamics of bacteria, protozoa, macroinvertebrates and amphibians. Bacterial concentration, in particular, is assumed not to limit remineralization and recycling, constituting a large pool which reacts rapidly to the availability of organic material. In this way, the role of bacteria is parameterized in the nutrient remineralization terms.

The limiting nutrient is assumed to be phosphorus, as is typical for most freshwater ecosystems. We expect phosphorus to be either organic and contained in living plankton cells, included in the detritus, or available as dissolved or colloidal organic phosphorus.

Another important limiting factor is light intensity, I, which is assumed to vary seasonally and also to be affected by the presence of high phytoplankton concentrations which can shadow the lower water layers.

We first consider the case of one vertically homogeneous lake water layer (such as happens for a fully mixed shallow lake, for example the Upper Trebecchi Lake at Gran Paradiso).

We denote by g_1, g_2, g_Z, g_F and g_C the growth efficiencies of the respective kinds of plankton and fish, i.e. the fraction of ingested food (or nutrient, for phytoplankton) used for biomass growth and reproduction. The fractions 1-g are instead used for metabolism. The parameters m_1, m_2, m_Z and m_F denote linear mortality rates of phytoplantkton, zooplankton and planktivorous fish respectively, and are assumed to be constant. Planktivorous fish is assumed to feed on zooplankton and to be subject to linear mortality. Piscivorous fish feed on planktivorous fish and are affected by quadratic mortality, representing also the feeding of carnivorous fish on its same compartment.

Nutrient

The dynamics of nutrient concentration is described by

$$\frac{dN}{dt} = -V_1 F_1(N,I)\, Q P_1 - V_2 F_2(N,I) Q P_2 + Q\rho + \Phi \tag{1.1}$$

where N denotes the concentration of bioavailable phosphorus, i.e. orthophosphate and other forms of organic or inorganic phosphorus that may be immediately utilized, and I is light intensity. The Liebig functions $F_i(N,I)$ are given below. The first term on the right-hand side of this equation describes phosphorus uptake and the parameters V_1 and V_2 are the maximal nutrient uptake rates by phytoplankton.

The carbon content of P_1 and P_2 is multiplied by the molar P:C ratio Q of phytoplankton, to obtain the phosphorus contained therein. Stoichiometric ratios in lakes do not generally obey Redfield ratios, and can differ between different species/groups (e.g., Andersen and Hessen 1991, Touratier et al. 2001, Vrede et al 2002, Reynolds 2006). For simplicity, here we assume a fixed P:C ratio of 1/100. Experimentation with different values do not lead to relevant variations in the results, especially because the regeneration terms play a very limited role in the high-nutrient conditions of the lakes considered here.

The term ρ indicates the remineralization rate of the organic phosphorus, implicitly representing the activity of bacteria. Phosphorus in the ecosystem comes from rapid recycling in the water column, in the form of release from plankton (secretion and waste during the growth process), and from rapid remineralization of dead organic matter in the water column (part of which is lost to the sediment). The term ρ is given explicitly in equation (1.9) discussed below. In the model, this contribution is added instantaneously to the P pool.

The parameter Φ is the external influx of soluble phosphorus, by rainfall, runoff or bottom resuspension. It can be a constant flux of nutrient, independent of the nutrient level inside the system, or a relaxation term (chemostat model) of the kind

$$\Phi = -\frac{N - N_0}{\tau}$$

where N_0 is the nutrient level in the chemostat and $1/\tau$ is the relaxation rate.

Phytoplankton

The model adopted here is developed for considering two different phytoplankton compartments, distinguished for example by their size (dinoflagellates versus diatoms) or by their nutrient uptake variability, or by their response to light. As discussed in the following, in general only one compartment of phytoplankton survives in the homogeneous model. However, we keep two compartments to allow for future explorations of very different conditions.

The equations for phytoplankton dynamics are

$$\frac{dP_1}{dt} = g_1 V_1 F_1(N,I)\, P_1 - r_Z\, G(P_1,P_2) \frac{\alpha P_1}{\alpha P_1 + (1-\alpha) P_2} Z - m_1 P_1 \tag{1.2}$$

$$\frac{dP_2}{dt} = g_2 V_2 F_2(N,I)\, P_2 - r_Z\, G(P_1,P_2) \frac{(1-\alpha) P_2}{\alpha P_1 + (1-\alpha) P_2} Z - m_2 P_2 \tag{1.3}$$

where P_1 and P_2 are the phytoplankton concentrations. In equations (1.2,1.3), the first term corresponds to growth of phytoplankton by nutrient uptake, the second term to loss of phytoplankton due to consumption by zooplankton. The third term represents linear phytoplankton mortality, which includes both natural mortality and the sinking of phytoplankton cells out of the water column.

The parameters V_1 and V_2 are the maximal nutrient uptake rates of phytoplankton. The parameter r_Z is the maximal grazing rate of zooplankton.

The functions F_1, F_2 are Liebig functions defined as

$$F_i(N,I) = \min\left\{\frac{N}{\kappa_i + N}, \frac{I}{\lambda_i + I}\right\} \quad , \quad i = 1,2. \tag{1.4}$$

The parameters κ_i and λ_i are the half-saturation constants for nutrient and light respectively. The two phytoplankton compartments may respond to lack of nutrient and/or light in different ways (i.e., have different values for κ_i and λ_i).

The parameter α represents the preference of zooplankton for the P_1 phytoplankton compartment and it depends on phytoplankton size and ability to form colonies and on general phytoplankton palatability. If zooplankton does not consume P_1, then α =0. If zooplankton does not consume P_2, then α =1.

The function $G(P_1,P_2)$ is a generalization of the Holling type-III functional form for predation over two compartments and it can be written as

$$G(P_1,P_2) = \frac{\left[\alpha P_1 + (1-\alpha)P_2\right]^2}{\varepsilon^2 + \left[\alpha P_1 + (1-\alpha)P_2\right]^2} \tag{1.5}$$

Zooplankton

The dynamical equation for zooplankton is

$$\frac{dZ}{dt} = g_Z r_Z G(P_1,P_2)Z - r_F \frac{Z^2}{\eta^2 + Z^2}F - m_Z Z \tag{1.6}$$

where the first term on the r.h.s. is zooplankton grazing on phytoplankton, the second term represents a Holling type-III predation of zooplankton by planktivorous fish (see Kot 2001 for an introduction to predation functional types and Sarnelle and Wilson 2008 for the case of *Daphnia*) and the third term is linear zooplankton mortality. The parameter r_Z is the maximal grazing rate of zooplankton and the function G has been defined in eq. (1.5). The parameter r_F is the maximal grazing rate of fish on zooplankton and □ is the saturation constant in the Holling type-III functional form.

Planktivorous fish

We assume that planktivorous fish feed on zooplankton. The dynamical equation for planktivorous fish is

$$\frac{dF}{dt} = g_F r_F \frac{Z^2}{\eta^2 + Z^2} F - r_C \frac{F^2}{\omega^2 + F^2} C - m_F F \tag{1.7}$$

where the first term represents fish grazing on zooplankton, the second term is planktivorous fish predation by piscivorous fish and the third term is linear mortality. The parameter r_F is the maximal grazing rate of zooplankton by planktivorous fish and r_C is the maximal grazing rate of piscivorous fish, again using a Holling type-III functional form.

Piscivorous fish

The dynamical equation for the piscivorous fish compartment is

$$\frac{dC}{dt} = g_C r_C \frac{F^2}{\omega^2 + F^2} C - d_C C^2 \tag{1.8}$$

where the first term is the growth of piscivorous fish by grazing on planktivorous fish and the second term is quadratic mortality, which includes a parametrization of piscivorous fish predation on its same compartment and mathematically allows for a finite value of piscivorous fish at equilibrium. The parameter r_C is the maximal grazing rate of planktivorous fish by piscivorous fish and d_C is the quadratic mortality parameter (having different units with respect to the linear mortality rates). See Steele and Henderson (1992) for a discussion of quadratic mortality.

Direct nutrient recycling

The fraction of food that is not used for biomass growth enters the metabolism of the consumer/predator. This biomass is then egested (i.e. respired, excreted, or secreted from the body surface). The phosphorus content of the egested biomass is assumed to be rapidly transformed into soluble, bioavailable phosphorus by the bacterial and enzymatic activity. This soluble reactive phosphorus is indicated by the term ρ and is added instantaneously to the nutrient compartment, see eq. (1.1).

The term ρ, representing direct nutrient recycling, is expressed as

$$\begin{aligned}\rho = \gamma_0 \Big[& (1-g_1) V_1 F_1(N,I)\, P_1 + (1-g_2) V_2 F_2(N,I)\, P_2 \\ & + (1-g_Z) r_Z G(P_1,P_2) Z + (1-g_F) r_F \frac{Z^2}{\eta^2 + Z^2} F + (1-g_C) r_C \frac{F^2}{\omega^2 + F^2} C \Big] \\ & + \gamma \left[m_1 P_1 + m_2 P_2 + m_F F + d_C C^2 \right]\end{aligned} \tag{1.9}$$

where $1\text{-}g_1$, $1\text{-}g_2$, $1\text{-}g_Z$, $1\text{-}g_F$ and $1\text{-}g_C$ indicate the fraction of resource/prey which is used for metabolism, $0 \le \gamma \le 1$ indicates the fraction of dead biomass which is remineralized in the water column before sinking into the bottom sediment and $0 \le \gamma_0 \le 1$ indicates the fraction of excreta which are remineralized in the water column.

Temperature dependence

Some of the parameters depends on temperature. For now, we consider only the temperature dependence of the phytoplankton growth rate, and use either a linear or a nonlinear form of temperature dependence, expressed as

$$V_i = V_{i,0}\, T / T_{\max} \qquad \text{linear}$$

$$V_i = V_{i,0}\, T / \left(\theta + T\right) \qquad \text{nonlinear} \tag{1.10}$$

Where $T_{\max}$ is the maximum temperature attained by the system for the linear case and □ is the hald-saturation constant for the nonlinear dependence. Previous results indicate the appropriateness of the nonlinear form (Thébault and Rabouille 2003).

Seasonal dependence

Light intensity and temperature are seasonally dependent. For light, we make the hypothesis that

$$I = I_0 + \left(I_{\max} - I_0\right)\left[1 - \cos\left(2\pi t / 365\right)\right] / 2 \tag{1.11}$$

so that light has a minimum I_0 on Dec 31 and a maximum $I_{\max}$ on June 30, with the agreement that the time t in days is $t = 1$ on Jan 1st of the first year of the simulation.

Temperature is expressed by a similar function,

$$T = T_0 + \left(T_{\max} - T_0\right)\left[1 - \cos\left(2\pi (t - \delta) / 365\right)\right] / 2 \tag{1.12}$$

where δ is a time delay due to the fact that seasonal temperature variation lags seasonal light intensity variation. In this way, temperature has an annual minimum on day δ.

Notice that, in the current formulation of the model, we consider only seasonal variation and do not take into account the daily or inter-annual variations in temperature, light intensity (cloudiness), nutrient influx or wind conditions (associated with mixing). For this reason, the comparison between model outputs and observations described in the following chapters should be taken as purely qualitative.

A simplified version of the above model, with fixed light intensity and valid only for the (ice-free) summers, was used to model the impact of introduced fish species (notably, the brook trout *Salvelinus fontinalis*) in the high-altitude lakes monitored in Gran Paradiso National Park (Magnea et al. 2013). Table 1 reports, as an example, the parameter values adopted for the highly-oligotrophic Alpine lakes of Gran Paradiso.

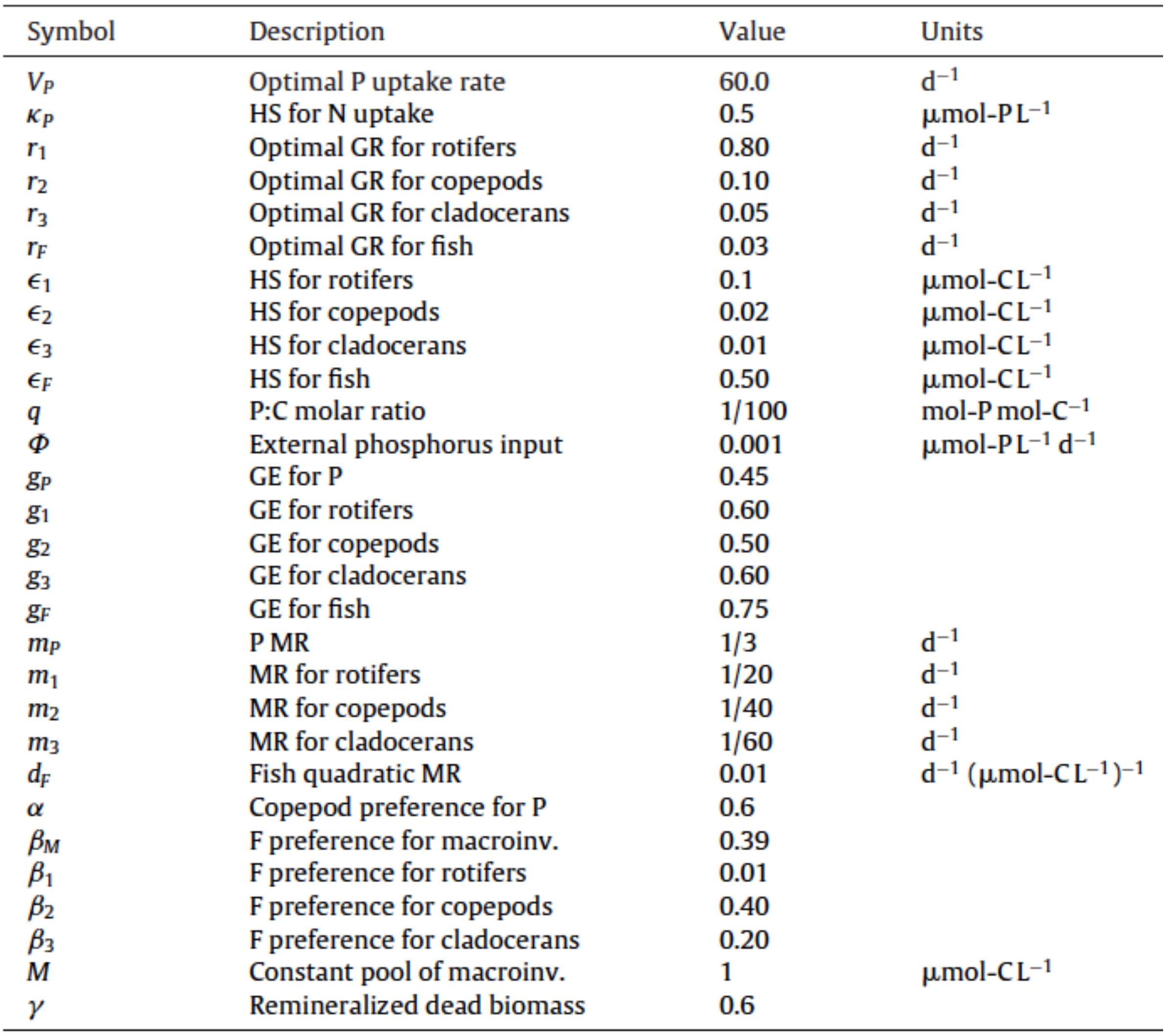

Symbol	Description	Value	Units
V_P	Optimal P uptake rate	60.0	d^{-1}
κ_P	HS for N uptake	0.5	μmol-P L^{-1}
r_1	Optimal GR for rotifers	0.80	d^{-1}
r_2	Optimal GR for copepods	0.10	d^{-1}
r_3	Optimal GR for cladocerans	0.05	d^{-1}
r_F	Optimal GR for fish	0.03	d^{-1}
ϵ_1	HS for rotifers	0.1	μmol-C L^{-1}
ϵ_2	HS for copepods	0.02	μmol-C L^{-1}
ϵ_3	HS for cladocerans	0.01	μmol-C L^{-1}
ϵ_F	HS for fish	0.50	μmol-C L^{-1}
q	P:C molar ratio	1/100	mol-P mol-C^{-1}
Φ	External phosphorus input	0.001	μmol-P L^{-1} d^{-1}
g_P	GE for P	0.45	
g_1	GE for rotifers	0.60	
g_2	GE for copepods	0.50	
g_3	GE for cladocerans	0.60	
g_F	GE for fish	0.75	
m_P	P MR	1/3	d^{-1}
m_1	MR for rotifers	1/20	d^{-1}
m_2	MR for copepods	1/40	d^{-1}
m_3	MR for cladocerans	1/60	d^{-1}
d_F	Fish quadratic MR	0.01	d^{-1} (μmol-C L^{-1})$^{-1}$
α	Copepod preference for P	0.6	
β_M	F preference for macroinv.	0.39	
β_1	F preference for rotifers	0.01	
β_2	F preference for copepods	0.40	
β_3	F preference for cladocerans	0.20	
M	Constant pool of macroinv.	1	μmol-C L^{-1}
γ	Remineralized dead biomass	0.6	

Table 1. Model parameters and their values for Gran Paradiso lakes. GE, growth efficiency; GR, growth rate; HS, half saturation constant; MR, mortality rate; P, phytoplankton; N, Phosphorus; F, fish. From Magnea et al (2013).

Stratified lakes

In case of a stratified lake, we consider a model system composed of two vertical layers, one above the thermocline (epilimnion) and one below (hypolimnion). The upper layer is characterized by abundant light while the lower layer is characterized by darker conditions.

Nutrient is supposed to enter the upper layer through a given external flux associated with the input of water streams and precipitation and leave the upper layer by a flux associated to water flow out of the lake. In this simplified formulation, we assume a given input flux Φ_0, independent of the nutrient concentration in the lake, and an output flux that depends linearly on the nutrient concentration in the lake, $-\beta N$. This choice relies on the assumption that there is an independent nutrient source from the water input, and a fixed water volume leaving the upper layer of the lake; thus, the loss of nutrient is proportional to the nutrient concentration N.

From the bottom, there is a nutrient input in the lower layer due to decomposition of organic material in the sediment and nutrient release from the chemostat represented by the nutrient-rich bottom sediment. This is obtained by using a relaxation term of the form $\Phi = -(N-N_0)/\tau$ where N_0 is the nutrient reservoir in the bottom.

There is an additional nutrient mixing term between the two layers, expressed as $\mu(N_2-N_1)$ for the upper layer and $\mu(N_1-N_2)$ for the lower layer, associated with turbulent exchanges between the two layers. Mixing is assumed to vary seasonally, from a maximum μ_0 in winter to a minimum in summer. For simplicity, we assume that the mixing intensity varies sinusoidally with time, with a delay δ_1 with respect to the temperature variation.

We assume that the excreta produced by the metabolism and the dead organic material sink to the bottom. There, it will participate in the nutrient reservoir of the bottom which re-enters the lower layer by the relaxation term.

Phytoplankton is split into two populations, P_1 and P_2, living respectively in the upper and lower layer. The parameters of the two populations are the same, but the temperature and the light level of the two layers are different. One can also include a mixing term between the two populations, i.e. a coupling term of the form $\mu_P(P_2-P_1)$ for the upper layer and $\mu_P(P_1-P_2)$ for the lower layer, due to turbulent mixing and/or phytoplankton vertical movements between the two layers. Here we assume that only turbulent mixing is active, and thus $\mu_P = \mu$.

Zooplankton are supposed to be able to freely move between the two layers and to feed on phytoplankton, wherever they are. Although visual predators may have a preference for the upper layer where light is more abundant and there is a diurnal cycle of zooplankton predation, we shall ignore these effects here. Consequently, only one compartment of zooplankton is kept in the model. Analogous behavior is assumed for fish.

The two-layer model has seven compartments, namely nutrient and phytoplankton in the upper and lower layer, zooplanton, planktivorous fish, and piscivorous fish. The equations are written as:

Zooplankton are supposed to be able to freely move between the two layers and to feed on phytoplankton, wherever they are. Although visual predators may have a preference for the upper layer where light is more abundant and there is a diurnal cycle of zooplankton predation, we shall ignore these effects here. Consequently, only one compartment of zooplankton is kept in the model. Analogous behavior is assumed for fish.

The two-layer model has seven compartments, namely nutrient and phytoplankton in the upper and lower layer, zooplanton, planktivorous fish, and piscivorous fish. The equations are written as:

$$\frac{dN_1}{dt} = -V(T_1)F(N_1,I_1)\,QP_1 + \Phi_0 - \beta N_1 - \mu(N_1 - N_2) \tag{1.13}$$

$$\frac{dN_2}{dt} = -V(T_2)F(N_2,I_2)\,QP_2 - \mu(N_2 - N_1) - \frac{N_2 - N_0}{\tau} \tag{1.14}$$

$$\frac{dP_1}{dt} = gV(T_1)F(N_1,I_1)\,P_1 - r_Z\,G(P_1,P_2)\frac{P_1}{P_1 + P_2}Z - mP_1 - \mu(P_1 - P_2) \tag{1.15}$$

$$\frac{dP_2}{dt} = gV(T_2)F(N_2,I_2)\,P_2 - r_Z\,G(P_1,P_2)\frac{P_2}{P_1 + P_2}Z - mP_2 - \mu(P_2 - P_1) \tag{1.16}$$

$$\frac{dZ}{dt} = g_Z r_Z\,G(P_1,P_2)Z - r_F\frac{Z^2}{\eta^2 + Z^2}F - m_Z Z \tag{1.17}$$

$$\frac{dF}{dt} = g_F r_F\frac{Z^2}{\eta^2 + Z^2}F - r_C\frac{F^2}{\omega^2 + F^2}C - m_F F \tag{1.18}$$

$$\frac{dC}{dt} = g_C\,r_C\frac{F^2}{\omega^2 + F^2}C - d_C C^2 \tag{1.19}$$

where the indices i=1,2 refer to the populations respectively in the upper and lower layer,

$$F(N_i,I_i) = \min\left\{\frac{N_i}{\kappa + N_i},\frac{I_i}{\lambda + I_i}\right\} \quad , \quad i = 1,2 \quad , \tag{1.20}$$

$$G(P_1,P_2) = \frac{[P_1 + P_2]^2}{4\varepsilon^2 + [P_1 + P_2]^2} \quad , \tag{1.21}$$

$$V(T) = V_0\,T/(\theta + T) \tag{1.22}$$

and T_1, T_2, I_1 and I_2 are respectively the temperature in the upper and lower layer and the light intensity in the upper and lower layer. For simplicity, we assume $I_2 = \xi I_1$ where ξ=exp(-H/D), H is related to the depth of the epilimnion and D is related to the extinction depth of light penetration. The seasonal variation of light intensity, temperature and mixing rate are written as

$$I_1 = I_0 + \left(I_{\max} - I_0\right)\left[1-\cos\left(2\pi t / 365\right)\right]/2 \quad , \quad I_2 = \xi I_1 \tag{1.23}$$

$$T_i = T_{i,0} + \left(T_{i,\max} - T_{i,0}\right)\left[1-\cos\left(2\pi (t-\delta) / 365\right)\right]/2 \quad , \quad i = 1,2 \tag{1.24}$$

$$\mu = \mu_0 + \left(\mu_1 - \mu_0\right)\left[1-\cos\left(2\pi (t-\delta-\delta_1) / 365\right)\right]/2 \tag{1.25}$$

The above models are written in Fortran and are available upon request.

References

Andersen, T. and D. O. Hessen, 1991. Carbon, nitrogen, and phosphorus content of freshwater zooplankton, Limnol. Oceanogr. 36, 807-814.

Bracco, A., A. Provenzale and I. Scheuring, 2000. Mesoscale vortices and the paradox of the plankton. Proc. R. Soc. B 267, 1795-1800.

Bratbak, G. and I. Dundas, 1984. Bacterial Dry Matter Content and Biomass Estimations. Applied and Environmental Microbiology, 48, 755-757.

Koszalka, I., A. Bracco, C. Pasquero and A. Provenzale, 2008. Plankton cycles disguised by turbulent advection. Theor. Pop. Biology 72, 1–6.

Kot, M. 2001. *Elements of Mathematical Ecology*, Cambridge University Press.

Magnea, U., Sciascia, R., Paparella, F., Tiberti, R., Provenzale, A. 2013. A model for high-altitude alpine lake ecosystems and the effect of introduced fish. Ecological Modelling 251, 211-220.

Martin, A., K.J. Richards, A. Bracco and A. Provenzale, 2002. Patchy productivity in the open ocean. Global Biogeochem. Cycles 16, 10.1029/2001GB001449.

Pasquero, C., A. Bracco and A. Provenzale, 2005. Impact of the spatiotemporal variability of the nutrient flux on primary productivity in the ocean. J. Geophys. Res. 110, C07005.

Reynolds, C.S., 2006. *Ecology of phytoplankton*, Cambridge University Press.

Sarnelle, O. and A.E. Wilson, 2008. Type-III functional response in Daphnia, Ecology, 89, 1723–1732.

Steele, J.H. and W. Henderson, 1992. The role of predation in plankton models. J. Plankton Res. 14, 152–172.

Straskrabová V., C. Callieri, P. Carrillo, L. Cruz-Pizarro, J. Fott, P. Hartman, M. Macek, J. M. Medina-Sánchez, J. Nedoma and K. Simek, 1999. Investigations on pelagic food webs in mountain lakes - aims and methods. Journal of Limnology 58, 77-87.

Thébault, J.M. and S. Rabouille, 2003. Comparison between two mathematical formulations of the phytoplankton specific growth rate as a function of light and temperature, in two simulation models (Aster& Yoyo). Ecological Modelling 163, 145-151.

Touratier, F., J. G. Field and C. L. Moloney, 2001. A stoichiometric model relating growth substrate quality (C:N:P ratios) to N:P ratios in the products of heterotrophic release and excretion, Ecological Modelling 139, 265-291.

Vrede, K., M. Heldal, S. Norland and G. Bratbak, 2002. Elemental composition (C, N, P) and cell volume of exponentially growing and nutrient-limited bacterioplankton, Applied and Environmental Microbiology, 68, 29652971.

Wetzel, R.G., 2001. *Limnology – Lake and River Ecosystems*, Elsevier Academic Press.

2. A conceptual model for the mountain Critical Zone

(Marta Magnani, CNR IGG; Antonello Provenzale, CNR IGG)

The Earth Critical Zone (CZ) is a relatively recent entry in the scientific landscape (see e.g. Giardino and Houser, 2015 for a detailed review). The term appeared for the first time in 1998 in an abstract by Ashley Gail (Ashley 1998), but only in 2001 a strict definition was proposed by the US NRC. The CZ is *"[…] the heterogeneous, near surface environment in which complex interactions involving rocks, soil, water, air and living organisms regulate the natural habitat and determine the availability of life sustaining resources."* (NRC Committee, 2001). The structure and processes that characterize the CZ influence the storage and fluxes of water, solute, gas, sediments, biota and energy providing an *ecosystem service* that is critical to life. According to the definition proposed above, the domain of CZ science extends from the top of the vegetation canopy down to the unperturbed bedrock, involving a broad range of disciplines and implying variable processes in spatial and temporal extension. The model we are going to present is embedded in the CZ framework; focusing on the water and vegetation roles in particular.

Water is the natural link between all the components involved: it travels from the atmosphere, through biota, to surface and deep soil; being a key component in soil weathering and sustenance of ecosystems. Moreover, in mountain areas the availability of water and the snow cover are the main limiting factors to biota development. They strictly control the plants growing cycle, and affect the gas exchanges with atmosphere as well as the whole trophic web (Jacobson et al., 2004, Portier et al. 1998). Then, the simplest conceptual model of the mountain CZ should account of the coupled water-vegetation dynamics, at least in the upper soil layer.

Here, we discuss the implementation of a coupled eco-hydrological box model for the local soil moisture and vegetation cover. In the following s will be the relative soil moisture, or just soil moisture averaged over a soil layer of depth Z_r and b the fraction of ground surface covered by vegetation. We will use an implicit-space description of the soil surface. The domain of the simulation is subdivided into neighboring sites which can be vegetated or empty. The total density of sites is set to 1 as well as the maximal soil moisture, thus the two simulated variables provide a fractional information (i.e. $b \in [0,1]$ and $s \in [0,1]$).

During the winter season, mountain areas are often covered by a (possibly rather thick) coat of snow. Under the snow the plant metabolic rates are significantly slowed down. On the other hand, (solid) precipitation accumulate on the top of the snow cover preventing liquid water from infiltration into the soil. Theoretically, the dynamics of vegetation and soil moisture is "frozen" during winter periods and the model reproduces such feature by maintaining b and s constant in winter. In this framework we neglect the contribution of the snowmelt to the infiltration (Zeinivand and De Smedt, 2009). Such assumption becomes even more solid when one studies the convergence time of the variables. Indeed, the vegetation varies on longer time scales and perturbations of the initial value $b(t = 0)$ take more than two decades to converge. The faster dynamics of the soil moisture make this variable to converge in tens of days.

The model described here below has been used in a preliminary study of the CZ Observatory established in 2017 at Nivolet Plain (CZO@Nivolet) in the Gran Paradiso National Park, Western Italian Alps. The daily precipitation (from 1962 onwards) recorded at a neighboring meteorological site was used as input. The model alternates growing seasons and frozen periods in which the soil is respectively free or covered with snow, reproducing the succession of summer and winter seasons. The numerical results were compared with in situ measurements of soil moisture, in order to analyze the water storage in soils with different geological origin. Note that the generality of the model allowed the application to quite dissimilar environments in past works. An example is the study of rainfall intermittency in arid lands presented by Baudena et al. in 2007. The model is written in Fortran 90 and it is available upon request.

Soil moisture

In this section we introduce the box-model for the total water content averaged over a given, active soil depth, i.e. the root zone Z_r. The model is suitable for application at local scale where the variable s has to be considered as the ratio between the number of soil pores filled by water and the total amount of pores within a reference volume. The vertical structure and the propagation of the wetting front are not included, i.e. the soil property and the soil moisture are considered to be uniform over the root zone.

At daily time scale the dynamics of the soil moisture consists in the global water balance between the water input due to rainfall, and subsequent infiltration, and the water losses due to evapotranspiration from vegetated soil, evaporation from bare soil and deep percolation, referred as leakage in the following (Laio et al, 2001). Thus one can write

$$\frac{\mathrm{d}s}{\mathrm{d}t} = \frac{1}{nZ_r}\,[I(s,r) - X(s,b)]\,, \tag{2.1}$$

where Z_r is the depth of the roots zone in millimeters (mm), n is the soil porosity, $I(s,r)$ the infiltration rate, with r the daily rainfall, and $X(s)$ the total water. Both infiltration and losses and daily rainfall units are millimeter of water per day (mm/day). Thus, from (2.1) one finds out that $\mathrm{d}t$ is measured in days.

In reality, evaporation (and evapotranspiration) are maintained as long as the specific humidity of soil (and plants) is larger than the air surface specific humidity (Williamson et al., 2006). During precipitation events the atmosphere is close to the saturation point and these processes are strongly weakened or stopped. Since we do not explicitly simulate the air moisture, we will assume infiltration and losses as mutually exclusive processes: infiltration is present only during those days when the daily cumulative precipitation is non-null while the losses are neglected and vice versa. The last assumption allowed us to solve eq. (2.1) alternatively for infiltration and losses with different methods: the first with a Eulerian integration of time step $dt/2$ and the second with a second order Runge-Kutta (RK2). The choice of the Eulerian step is dictated by the fact that eq. (2.1) is coupled with the equation for vegetation dynamics, described in the following, that is solved with RK2 methods and the last need the value of soil water at the half step (see e.g. Press et al, 1996 and reference therein). As an example, in the CZO@Nivolet study we employed a time step of 1 hour, corresponding to $dt = \frac{1}{24}day$. There, we directly measure the Volumetric Water Content (VWC) of different soils, that is $VWC = s\,n$ (Rodriguez_Iturbe and Portporato, 2005); once known the soil porosity one can easily convert the numerical results for the comparison with data.

Evaporation, evapotranspiration and leakage

Eq. (2.1) is an Ordinary Differential Equation (ODE) that hides non-linearity in the term of water losses. The explicit expression for the total loss reads (Laio et al, 2001)

$$X(s,b) = b\,[ET(s) + L(s)] + (1-b)[E(s) + L(s)], \tag{2.2}$$

where the vegetation and soil moisture dependences factorize through the functions of evapotranspiration (ET), evaporation (E) and leakage (L). The water loss from the vegetated sites is given by $ET(s) + L(s)$ and its contribution to the total loss is weighted by the fraction of vegetated sites, b. The bare soil can lose water by evaporation and leakage, $E(s) + L(s)$, and only the non-vegetated sites, whose fraction is $1 - b$, contribute. All the three functions in (2.2) are piecewise defined functions and depend on moisture thresholds. These are

$$ET(s) = \begin{cases} 0 & \text{if } s \leq s_h \\ E_w \dfrac{s - s_h}{s_w - s_h} & \text{if } s_h < s \leq s_w \\ E_w + (E_{max} - E_w)\dfrac{s - s_w}{s^* - s_w} & \text{if } s_w < s \leq s^* \\ E_{max} & \text{if } s^* < s \leq 1 \end{cases} \tag{2.3}$$

$$E(s) = \begin{cases} 0 & \text{if } s \leq s_h \\ E_w \dfrac{s - s_h}{s_w - s_h} & \text{if } s_h < s \leq s_{fc} \\ E_w \dfrac{s_{fc} - s_h}{s_w - s_h} & \text{if } s_{fc} < s \leq 1 \end{cases} \tag{2.4}$$

$$L(s) = \begin{cases} 0 & \text{if } s \leq s_{fc} \\ K_s \dfrac{e^{\beta(s - s_{fc})} - 1}{e^{\beta(1 - s_{fc})} - 1} & \text{if } s > s_{fc} \end{cases} \tag{2.5}$$

For typical values of the parameter E_{max}, E_w, K_s, β and soil moisture thresholds s_h, s_w, s^*, s_{fc} we refer to Table 2. A detailed derivation of the parameters for different textures can be found e.g. in Rodriguez-Iturbe and Porporato, 2005 and references therein.

In a given habitat, a constant transpiration rate E_{max} occurs at optimal conditions ($s \geq s^*$). Below the critical value of s^*, plants start (linearly) reducing transpiration by closing their stomata. If the soil moisture drops further, below the wilting point s_w, the water stress forces the plants to completely close their stomata and progressively wilt. Only evaporation contributes to water depletion below this threshold. Here, the value of evaporation at the wilting point is marked as E_w. Finally, the model assumes that below the hygroscopic point no evaporation takes place. Thus, the value $s = 0$ is never actually achieved in the model. Ideally, below s_h the soil skin moisture is so low that it acts as a seal for the underlying water, then the average moisture is always non-null ($s > 0$).

Evaporation from bare soil follows simpler dynamics, since it increases linearly from the hygroscopic point up to its maximal value at the field capacity, s_{fc}. Below the wilting point the dynamics of bare and vegetated soil should match, as evapotranspiration reduces to pure evaporation. This condition justifies the presence of s_w and E_w in (2.4). However, above the wilting point the magnitude of evaporation is always lower than the evapotranspiration one, tending to the same limit when s goes to 1, where leakage dominates.

Leakage is the water percolation toward larger depth due to the action of the gravitational force on the liquid water and it is usually negligible except when the soil moisture exceeds the field capacity. In (2.5) such process is modeled by an exponential function that tends to the saturated hydraulic conductivity K_s as $s \to 1$.

Note that, since $X(s,b)$ is the rate of moisture depletion of soil within the time step dt, its dependence on the soil moisture results as a negative feedback. Higher soil moisture corresponds to larger water losses by evaporation and transpiration, that results in a stronger decrease of the soil moisture itself.

	n	s_h	s_w	s^*	s_{fc}	K_s (mm/d)	β
Sand	0.35	0.08	0.11	0.33	0.35	2000	12.1
Loamy sand	0.42	0.08	0.11	0.31	0.52	1000	12.7
Loam	0.45	0.19	0.24	0.57	0.65	200	14.8
Clay	0.50	0.47	0.52	0.78	0.99	90	26.8

Table 2. Examples of model parameter for different soil textures. The maximal value of evapotranspiration and evaporation at the wilting point are texture independent, i.e. $E_{max} = 4.5\ mm/d$ and $E_w = 0.1\ mm/d$ respectively.

Infiltration

The infiltration rate at the top layer of soil is directly determined by the rainfall rate. Here the cumulative daily precipitation is assumed to be uniformly distributed over the whole day. In each time step the amount of rainfall given by $r\Delta t$ infiltrates as follows (Laio et al, 2001)

$$I = \begin{cases} \dfrac{r}{nZr} & \text{if } \dfrac{r\Delta t}{nZr} < 1 - s \\ \dfrac{1-s}{\Delta t} & \text{if } \dfrac{r\Delta t}{nZr} \geq 1 - s \end{cases} \quad . \tag{2.6}$$

All the rainfall infiltrates as long as the soil is unsaturated. When this condition is not satisfied, the soil saturates and the water in excess is lost as surface runoff. Here, we assumed statistical homogeneity of rainfall in the domain of simulation and rapid water redistribution by surface runoff. As discussed above, we choose $r\Delta t = dt/2$ due to the coupling with the vegetation dynamics, that is solved with a second order RK2 method.

Vegetation cover

The dynamics of vegetation is described by a logistic equation (Levins, 1969), which was used to describe plant competition by Tillman (1994). In this approach, the fraction of occupied sites is determined by the colonization ability of plants and their mortality. Averaging the single parcel process over the whole domain one obtains the evolution equation for the fraction of occupied sites, i.e. the fraction of vegetation cover b, that is

$$\frac{\mathrm{d}b}{\mathrm{d}t} = \mathrm{g(s)}\ b(1-b) - \mu(s)b\,, \tag{2.7}$$

with

$$g(s) = \frac{g_0}{2}\left[1 + \tanh\left(\frac{s-s*}{a}\right)\right] \tag{2.8}$$

$$\mu(s) = \frac{\mu_1+\mu_2}{2} + \frac{\mu_1-\mu_2}{2}\ \tanh\left(\frac{s_w-s}{a}\right). \tag{2.9}$$

Here, $\mathrm{g}(s)$ is the colonization rate and $\mu(s)$ the extinction rate at local scale, in d^{-1}. They both depend on soil water thorough a steep hyperbolic tangent, whose steepness is given by the parameter a=0.002.

In (2.8) the hyperbolic tangent is centered on s*, the fully-open-stomata threshold of soil moisture. The colonization rate is assumed to be negligible, i.e. close to zero, when $s < s *$, while it tends to the optimal colonization rate $g_0 = 0.8\ \mathrm{y}^{-1}$ above this threshold. Thus, we coarsely model the scarce ability of plants to reproduce when the available water is lower than the optimal value, both because the water stress forces the plants to allocate fewer resources to seed production, and because seeds have lower germination probability when the soil is not sufficiently moist.

The extinction rate, i.e. the vegetation mortality, reaches its maximum $\mu_1 = 0.2\ \mathrm{y}^{-1}$ below the wilting point and it is minimal, tending to $\mu_2 = 0.1\ \mathrm{y}^{-1}$, above this threshold. The dependence on soil moisture is given by a reversed hyperbolic tangent centered on the wilting point for vegetation, s_w.

The overall dynamics of equation (2.7) accounts for the plant abundance and the soil moisture, through $\mu(s)$ and $g(s)$. Indeed, the propagule production rate is given by the product gb and it is weighted by the number of available sites $(1-b)$. This means that the larger is the number of occupied sites, the higher is the seeds production and the probability of appearance of new beings. The seeds are assumed to be randomly and uniformly spread over the whole habitat. However, the spreading of plants cannot be unlimited. The growth saturates due to the factor $(1-b)$, since a new plant established in an already occupied site does not change the number of occupied sites. Plants can also die by themselves according to the second term in (2.7), and the probability that an occupied sites become vacant is proportional to the plant abundance. Note that in this model the competition between individuals for resources is not explicitly modeled, i.e. production and mortality rate are density-independent. However, a larger population corresponds to higher evapotranspiration rates and a quicker depletion of resources. In ideal conditions of ever ending and constant supplies, b tends to an asymptotic value, that is directly determined by the maximal available water.

The above model is particularly suitable for studies of rainfall intermittencies (Baudena et al. 2007, Baudena and Provenzale 2008) and was adopted to explain the vegetation-type latitudinal gradient with the mean annual rainfall (D'Onofrio et al. 2015)

References

Ashley, G.M., 1998. Where are we headed? “Soft” rock research into the new millennium. *Geological Society of America Abstract/Program*, vol. 30. p. A-148.

Baudena, M., Boni, G., Ferraris, L., Von Hardenberg, J., and Provenzale, A. (2007). Vegetation response to rainfall intermittency in drylands: Results from a simple ecohydrological box model. *Advances in Water Resources*, *30*(5), 1320-1328

Baudena, M., & Provenzale, A. (2008). Rainfall intermittency and vegetation feedbacks in drylands. *Hydrology and Earth System Sciences Discussions*, *12*(2), 679-689.

D'Onofrio, D., Baudena, M., D'Andrea, F., Rietkerk, M., & Provenzale, A. (2015). Tree-grass competition for soil water in arid and semiarid savannas: The role of rainfall intermittency. *Water Resources Research*, *51*(1), 169-181.

Giardino, J. R., and Houser, C. (2015). *Principles and dynamics of the critical zone* (Vol. 19). Elsevier.

Jacobson, A. R., Provenzale, A., von Hardenberg, A., Bassano, B., & Festa-Bianchet, M. (2004). Climate forcing and density dependence in a mountain ungulate population. *Ecology*, *85*(6), 1598-1610.

Laio, F., Porporato, A., Ridolfi, L., and Rodriguez-Iturbe, I. (2001). Plants in water-controlled ecosystems: active role in hydrologic processes and response to water stress: II. Probabilistic soil moisture dynamics. *Advances in Water Resources*, *24*(7), 707-723.

Levins, R. (1969). Some demographic and genetic consequences of environmental heterogeneity for biological control. *American Entomologist*, *15*(3), 237-240.

National Research Council Committee on Basic Research Opportunities in the Earth Sciences, 2001. Basic Research Opportunities in the Earth Sciences. *National Academies Press*, Washington, DC.

Portier, C., Festa-Bianchet, M., Gaillard, J. M., Jorgenson, J. T., & Yoccoz, N. G. (1998). Effects of density and weather on survival of bighorn sheep lambs (Ovis canadensis). *Journal of Zoology*, *245*(3), 271-278.

Press, W. H., Teukolsky, S. A., Vetterling, W. T., & Flannery, B. P. (1996). *Numerical recipes in Fortran 90* (Vol. 2, pp. 402-408). Cambridge: Cambridge university press.

Rodríguez-Iturbe, I., and Porporato, A. (2005). *Ecohydrology of water-controlled ecosystems: soil moisture and plant dynamics*. Cambridge University Press.

Tilman, D. (1994). Competition and biodiversity in spatially structured habitats. *Ecology*, *75*(1), 2-16.

Williamson, M. S., Lenton, T. M., Shepherd, J. G., & Edwards, N. R. (2006). An efficient numerical terrestrial scheme (ENTS) for Earth system modelling. *Ecological Modelling*, *198*(3-4), 362-374.

Zeinivand, H., & De Smedt, F. (2009). Hydrological modeling of snow accumulation and melting on river basin scale. *Water resources management*, *23*(11), 2271-2287.

3. Empirical population dynamics models

(Antonello Provenzale, CNR IGG; Simona Imperio, ISPRA; Ramona Viterbi, PNGP)

In the framework of the NextData project and based upon the expertise developed in the last twenty years, we have developed a suite of data-based empirical models for the population dynamics of selected species (mainly, ungulates and tetraonids), see for example Jacobson et al. (2004), Imperio et al. (2012, 2013), Mignatti et al. (2012), Viterbi et al. (2014).

The models are built upon the knowledge of the time series of census counts of the total population, N_t, where N is the density (number in a selected area) of the individuals of the species considered (for example, number of chamois in the Gran Paradiso Park), and t indicates the year. In this application, we consider annual census counts (appropriate for species that reproduce once a year), and discrete time (that is, annual censuses).

The general dependence of the population fluctuations is described by the expression

$$N_{t+1} = F(N_t, N_{t-1}, \ldots , C_t, C_{t-1}, \ldots, N_t C_t, \ldots) , \tag{3.1}$$

where C_t represents a generic climate or environmental variable in year t. Examples are the average temperature, the summer precipitation, the winter snow cover, etc.

In general, the problem is to determine the form of F and what are the variables that are significant to explain a large fraction of the variance of the population fluctuations. If there is significant dependence on the previous-year population density (N_{t-1}), one can speak of direct density dependence. If there is a significant dependence on the population density from the previous years (N_{t-2} and before), one speaks of delayed density dependence. Same issue for the environmental variables: they can measure environmental conditions between the census of year $t-1$ and year t, or previous conditions that can have a delayed effect on the population.

In case the age (or stage) structure of the population is known, the models can reproduce the number (or density) of individuals in a given age class. For the cases of Alpine ibex (*Capra ibex*) and chamois (*Rupicapra rupicapra*) at Gran Paradiso, we implemented a stage-structured model including the dynamics of newborns (K), yearlings (Y) and adult males and females (M and F respectively), thanks to the availability of the corresponding empirical data. In such case, the model equations can be written as

$$M_{t+1} = S_M(N_t, N_{t-1}, \ldots , C_t, C_{t-1}, \ldots, N_t C_t, \ldots) (M_t + Y_t / 2) \tag{3.2}$$

$$F_{t+1} = S_F(N_t, N_{t-1}, \ldots , C_t, C_{t-1}, \ldots, N_t C_t, \ldots) (F_t + Y_t / 2) \tag{3.3}$$

$$Y_{t+1} = S_K(N_t, N_{t-1}, \ldots , C_t, C_{t-1}, \ldots, N_t C_t, \ldots) K_t \tag{3.4}$$

$$K_{t+1} = \Phi(N_t, N_{t-1}, \ldots , C_t, C_{t-1}, \ldots, N_t C_t, \ldots) F_{t+1} \tag{3.5}$$

where S_M, S_F and S_K are the survivals of adult males, females and of kids respectively, and Φ is the natality (number of newborns per survived female). In the above equations, we have assumed that the survival of yearling from their first to second year is the same as that of adults, and that there an equal gender balance in yearlings.

Also in this case the relevant issues are (a) to determine the functional form of the survivals and natality, either by a priori or a posteriori (data-based) considerations, and (b) to identify the significant explanatory variables. For these purposes, a variety of statistical methods are available, and have been implemented in the modelling system.

In most approaches, we have implemented regression-based Generalized Linear Models, with the inclusion – when appropriate – of multiplicative terms such as $N_t C_t$ or quadratic terms such as C_t^2. Delayed density dependence has also been included and tested. In the case of Alpine fauna, the main control variables for the considered cases have been identified as average depth of the snow cover, duration of the snow cover, start and end date of the snow cover, and spring precipitation (for the case of black grouse, *Tetrao tetrix*). Overall, the cases considered confirmed the fundamental role played by snow cover in the population dynamics of mountain fauna.

All models have been implemented in R language, Fortran and/or Matlab, and are available upon request.

References

Imperio, S., Focardi, S., Santini, G., Provenzale, A. 2012. Population dynamics in a guild of four Mediterranean ungulates: density-dependence, environmental effects and inter-specific interactions. Oikos, 121, 1613-1626.

Imperio, S., Bionda,R., Viterbi, R., Provenzale, A. 2013. Climate Change and Human Disturbance Can Lead to Local Extinction of Alpine Rock Ptarmigan: New Insight from the Western Italian Alps. PLOS ONE, 8, e81598. doi:10.1371/journal.pone.0081598.

Jacobson, AR, Provenzale, A., von Hardenberg, A., Bassano, B., Festa-Bianchet, M. 2004. Climate forcing and density dependence in a mountain ungulate population. Ecology, 85, 1598-1610.

Mignatti, A., Casagrandi, R., von Hardenberg, A., Gatto, M., Provenzale, A. 2012. Sex- and age-structured models for Alpine ibex *Capra ibex ibex* population dynamics. Wildlife Biology, 18, 318-332 (2012).

Viterbi, R., Imperio, S., Alpe, D., Bosser-Peverelli, V., Provenzale, A. 2014. Climatic Control and Population Dynamics of Black Grouse (*Tetrao tetrix*) in the Western Italian Alps. The Journal of Wildlife Management, doi: 10.1002/jwmg.810.